Close mass balance of long-term carbon fluxes from ice-core CO_2 and ocean chemistry records

RICHARD E. ZEEBE[1]* AND KEN CALDEIRA[2]

[1]School of Ocean and Earth Science and Technology, Department of Oceanography, University of Hawaii at Manoa, 1000 Pope Road, MSB 504, Honolulu, Hawaii 96822, USA

[2]Department of Global Ecology, Carnegie Institution, 260 Panama Street, Stanford, California 94305, USA

*e-mail: zeebe@soest.hawaii.edu

Published online: 27 April 2008; doi:10.1038/ngeo185

Feedbacks controlling long-term fluxes in the carbon cycle and in particular atmospheric carbon dioxide are critical in stabilizing the Earth's long-term climate. It has been hypothesized that atmospheric CO_2 concentrations over millions of years are controlled by a CO_2-driven weathering feedback that maintains a mass balance between the CO_2 input to the atmosphere from volcanism, metamorphism and net organic matter oxidation, and its removal by silicate rock weathering and subsequent carbonate mineral burial[1–4]. However, this hypothesis is frequently challenged by alternative suggestions, many involving continental uplift and either avoiding the need for a mass balance or invoking fortuitously balanced fluxes in the organic carbon cycle[5–9]. Here, we present observational evidence for a close mass balance of carbon cycle fluxes during the late Pleistocene epoch. Using atmospheric CO_2 concentrations from ice cores[10–12], we show that the mean long-term trend of atmospheric CO_2 levels is no more than 22 p.p.m.v. over the past 610,000 years. When these data are used in combination with indicators of ocean carbonate mineral saturation to force carbon cycle models, the maximum imbalance between the supply and uptake of CO_2 is 1–2% during the late Pleistocene. This long-term balance holds despite glacial–interglacial variations on shorter timescales. Our results provide support for a weathering feedback driven by atmospheric CO_2 concentrations that maintains the observed fine mass balance.

Carbon dioxide is released from volcanism and metamorphism to the atmosphere at a rate that would double the amount of carbon in the combined ocean–atmosphere system within less than 600 kyr (refs 13,14). Chemical weathering of Ca and Mg silicate rocks followed by carbonate burial removes CO_2 from the atmosphere through weathering reactions. The weathering rates of the silicate rocks increase with soil CO_2 concentration and temperature[15]. The long-term balance between carbon release and removal has been hypothesized to be maintained by a negative stabilizing feedback, which results from the influence of the partial pressure of atmospheric CO_2 on the Earth's surface temperature and silicate rock weathering rates[1–4]. Note that there are different types of this feedback, for example, before and after the rise of land plants[16]. If the rate of carbon input to the ocean–atmosphere system would exceed the rate of chemical weathering, atmospheric CO_2 and temperature would rise, thereby elevating weathering rates until a new balance is achieved and vice versa. Thus, CO_2 levels over millions of years would be controlled by a CO_2-driven weathering feedback that maintains a mass balance between CO_2 input to and removal from the atmosphere.

One school of thought has promoted this feedback as a key player in the long-term stabilization of the Earth's climate[16–18]. However, this view is controversial and frequently challenged by conflicting hypotheses. These hypotheses often involve continental uplift and avoid the need for a mass balance or postulate organic carbon fluxes that coincidentally balance the cycle[5–9]. Until present, the advocates of the weathering feedback have theoretically argued that CO_2 would undergo large variations within a few million years, if the feedback was absent[19,20]. Unfortunately, the mechanism is difficult to prove, partly because the involved fluxes cannot be measured directly over millions of years. As a result, the CO_2-driven weathering feedback, which has probably prevented runaway greenhouse and icehouse conditions over timescales of millions to billions of years, remains speculative.

To provide observational constraints on long-term carbon fluxes, we have turned to recently generated ice-core CO_2 records, now covering 650 kyr of the late Pleistocene epoch[12]. Previous studies have focused on analysing the causes of the glacial–interglacial variations. However, despite variations on the timescale of thousands of years, there is remarkably little trend on the timescale of hundreds of thousands of years. Here, we show that the lack of a strong trend in atmospheric CO_2 or ocean chemistry over this time period implies a tight coupling between CO_2 sources to and sinks from the atmosphere and oceans.

We have analysed Antarctic ice-core CO_2 records spanning the past 650 kyr (refs 10–12) (Fig. 1). The calculated linear, long-term trends in CO_2 based on different fit models (see the Methods section) range from -22 ± 2 p.p.m.v to $+10 \pm 6$ p.p.m.v. per 610 kyr (Table 1). In other words, the mean, long-term atmospheric CO_2 change during the past 610 kyr is at most 22 p.p.m.v. Superimposed on this trend are the well-known glacial–interglacial variations. In general, causes for a mean pCO_2 change can be split into two categories (see Supplementary Information, Fig. S1). (i) 'Surface recycling': a redistribution of carbon between or within surficial reservoirs of ocean (inventory $= M_C^{ocn}$), atmosphere (M_C^{atm}) and terrestrial biosphere (M_C^{trr}), with total carbon inventory M_C^S (refs 13,14):

$$M_C^S = M_C^{ocn} + M_C^{atm} + M_C^{trr} \simeq 40{,}000\ \mathrm{Pg\,C}. \qquad (1)$$

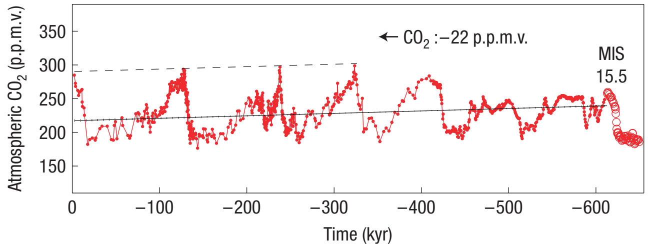

Figure 1 Late Pleistocene CO_2 records. The red curve shows combined data from Antarctic ice cores at Dome C and Vostok[10–12]. Open circles indicate data excluded from the truncated data sets (see Table 1). MIS: marine isotope stage. Solid black lines indicate long-term trends and errors based on linear regression of the truncated, interpolated data sets. The same trend in CO_2 shifted vertically (dashed line) shows that maximum values have also declined during the past four interglacials.

Table 1 Linear CO_2 trends (p.p.m.v. per 610 kyr) based on different fit methods. Results for all data (time interval = 647 kyr) are scaled to that of the truncated data set (610 kyr).

Data	$\Delta t \rightarrow$ Fit →	Original* Linear	Original* +Periodic‡	Interpolated† Linear	Interpolated† +Periodic‡
All		$+10 \pm 6$ §	$+5 \pm 5$	-12 ± 2	-12 ± 2
Truncated		$+0 \pm 6$	-4 ± 6	-22 ± 2	-21 ± 2

*Δt = time interval between individual ice-core measurements.

† Δt = time interval on linear time axis for interpolated values (Δt = const.).

‡Fit model: $a + bt + \sum c_j \cos[\omega_j(t - t_j)]$, see equation (8) of the Methods section.

§ Fit errors at 95% confidence interval (MATLAB curve fitting toolbox).

(ii) ‘Endogenic imbalance’: an imbalance between long-term carbon-cycle fluxes among endogenic reservoirs of mantle and upper crust involving volcanism/metamorphism, weathering and deep burial. In the case of surface recycling, M_C^S stays constant, whereas in the case of an endogenic imbalance, M_C^S is not constant.

The long-term trends in the CO_2 data (Table 1) can be due to surface recycling or an endogenic imbalance, or both. However, if only surface recycling was responsible, then long-term fluxes were in perfect balance. In the following we will therefore examine the case that the pCO_2 change was entirely due to an endogenic imbalance, which provides a maximum estimate for the mismatch between long-term carbon fluxes. If surface recycling was involved, then a finer balance is possible. For a given change in atmospheric CO_2 (ΔpCO_2), changes in the combined ocean–atmosphere inventory can then be constrained (for terrestrial biosphere, see Supplementary Information). We calculate the endogenic imbalance from mass balances of carbon and alkalinity (see Supplementary Information, Fig. S1); stable carbon isotopes merely constrain partitioning of net degassing and organic carbon oxidation:

$$M_C^T = M_C^{ocn} + M_C^{atm} \tag{2}$$

$$\frac{dM_C^T}{dt} = +F_{cw} - F_{cb} + F_{vm} + F_{gw} - F_{gb} \tag{3}$$

$$\frac{dM_A^T}{dt} = +2\,F_{cw} - 2\,F_{cb} + 2\,F_{sw} \tag{4}$$

$$\frac{d(\delta_C^T\, M_C^T)}{dt} = +\delta_{cw}\, F_{cw} - (\delta_C^T + \varepsilon_c)\, F_{cb} + \delta_{vm}\, F_{vm} + \delta_{gw}\, F_{gw} - (\delta_C^T + \varepsilon_g)\, F_{gb}, \tag{5}$$

where M_C^T is the total ocean–atmosphere carbon inventory (equation (1)), M_A^T is the alkalinity inventory and F terms are fluxes of $CaCO_3$ weathering/burial (cw/cb), volcanism/metamorphism (vm), organic carbon (C_{org}) weathering/burial (gw/gb) and silicate weathering (sw); δ terms refer to carbon isotope compositions (δ_C^T is the δ-value of M_C^T) and ε terms refer to fractionation factors; $[\delta_{cw}, \delta_{vm}, \delta_{gw}] = [+2, -1, -22]‰$ and $[\varepsilon_c, \varepsilon_g] = [+2, -25]‰$ (ref. 13). For any pair of initial and final pCO_2 and, for example, carbonate ion concentration ($[CO_3^{2-}]$), M_C^T and M_A^T and their time derivatives can be calculated[21], whereas changes in δ_C^T are determined from $\delta^{13}C$ records in benthic foraminifera (see the Supplementary Information). Thus, given input values of F_{cw}, F_{vm} and F_{gw} (refs 13,16,19), the system can be solved for the unknowns F_{cb}, F_{gb} and F_{sw} (equations (2)–(5)). Finally, the imbalance between CO_2 input to the atmosphere from volcanism/metamorphism and net C_{org} oxidation, and CO_2 uptake by silicate weathering, $I_{(inp-sw)}$, is given by:

$$I_{(inp-sw)} = (F_{vm} + F_{gw} - F_{gb}) - F_{sw} \tag{6}$$

$$I'_{(inp-sw)} = I_{(inp-sw)} / (F_{vm} + F_{gw}), \tag{7}$$

where $I'_{(inp-sw)}$ is the imbalance relative to the sum of the input fluxes $F_{vm} + F_{gw}$. Note that potential effects of terrestrial biomass changes on I' are small and that I' is independent of the carbon isotope balance (equation (5)) and thus of isotopic compositions and fractionation factors (see the Supplementary Information). As a result, our imbalance does not depend on the carbon isotope value of buried organic carbon, for instance, or changes in the long-term partitioning of organic carbon burial between marine and terrestrial environments (with generally different isotopic values).

Given the long-term CO_2 trends from our data analysis (Table 1), values for the imbalance over the past 610 kyr can now be calculated. For example, if pCO_2 drops from 240 to 218 μatm at constant $[CO_3^{2-}] = 224\ \mu mol\ kg^{-1}$, $I_{(inp-sw)}$ is equivalent to a loss of $42\ \mu mol\ kg^{-1}$ in total dissolved inorganic carbon (C_T) in the ocean at temperature and salinity of $T = 18\ °C$ and $S = 35$ (Fig. 2). In this case, loss of surficial carbon reduces C_T and pCO_2, which would also tend to increase $[CO_3^{2-}]$ and thus the $CaCO_3$ saturation state. However, the latter is effectively buffered by a process called calcite compensation[22,23], which restores $[CO_3^{2-}]$ on a timescale of ∼10 kyr. Thus, because $[Ca^{2+}]$ variations are small on glacial–interglacial timescales, at constant depth of the saturation horizon, C_T and pCO_2 decline along a line of $[CO_3^{2-}]$ = const. (Fig. 2, blue line). After calcite compensation, the calculated carbon loss from the ocean due to flux imbalances is $42\ \mu mol\ kg^{-1}$ (red line). A further $36\ \mu mol\ kg^{-1}$ is lost owing to excess $CaCO_3$ burial (green line). The flux-driven loss for the 22 μatm decline in pCO_2 corresponds to a 2.2% drop in C_T or a 840 Pg C loss relative to the combined ocean–atmosphere inventory of $M_C^T \simeq 36{,}500$ Pg C (ref. 14). Using $F_{vm} = 0.06$–$0.10\ Pg\,C\,y^{-1}$ and $F_{gw} = 0.06$–$0.12\ Pg\,C\,y^{-1}$ (refs 13, 16,19), the total input fluxes equal 73,200–134,200 Pg C and the total loss of 840 Pg C is equivalent to a relative imbalance of $I'_{(inp-sw)} = -0.6\%$ to -1.2% over 610 kyr ($\Delta pCO_2 = -22$ μatm). We found that varying temperature and salinity had little effect on I' (±0.004% for $T = 13$–$23\ °C$ and $S = 33$–37).

If we allow for simultaneous trends in the saturation horizon depth, $I'_{(inp-sw)}$ can be slightly larger or smaller, depending on the sign of $\Delta[CO_3^{2-}]$ (Fig. 3). If a pCO_2 drop is accompanied by a $[CO_3^{2-}]$ decrease, that is, a shallowing of the saturation

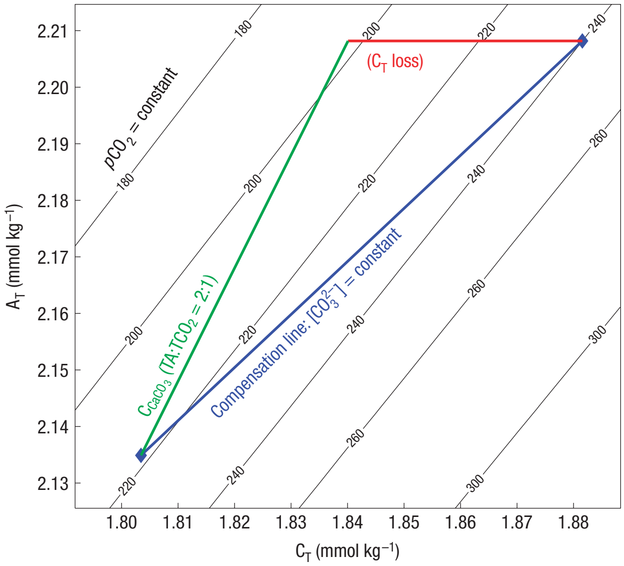

Figure 2 Example calculation of the imbalance between long-term carbon fluxes. The imbalance is calculated as the difference between input from volcanism/metamorphism plus net C_{org} oxidation and silicate weathering (C_T loss) for the case that a long-term trend in CO_2 is entirely due to an 'endogenic imbalance' (see equation (6)). Labelled black lines are pCO$_2$ contours (μatm) as a function of total dissolved inorganic carbon (C_T) and total alkalinity (A_T) in the ocean. At constant carbonate ion concentration ([CO_3^{2-}]), the pCO$_2$ drop (here from 240 to 218 μatm) occurs along the compensation line (blue). The reduction of pCO$_2$ and ocean inventories is composed of two steps: the actual loss of carbon due to the imbalance (red line) and subsequent calcite compensation, that is, precipitation of $CaCO_3$ reducing ocean C_T and A_T in a ratio of 1:2 (green line).

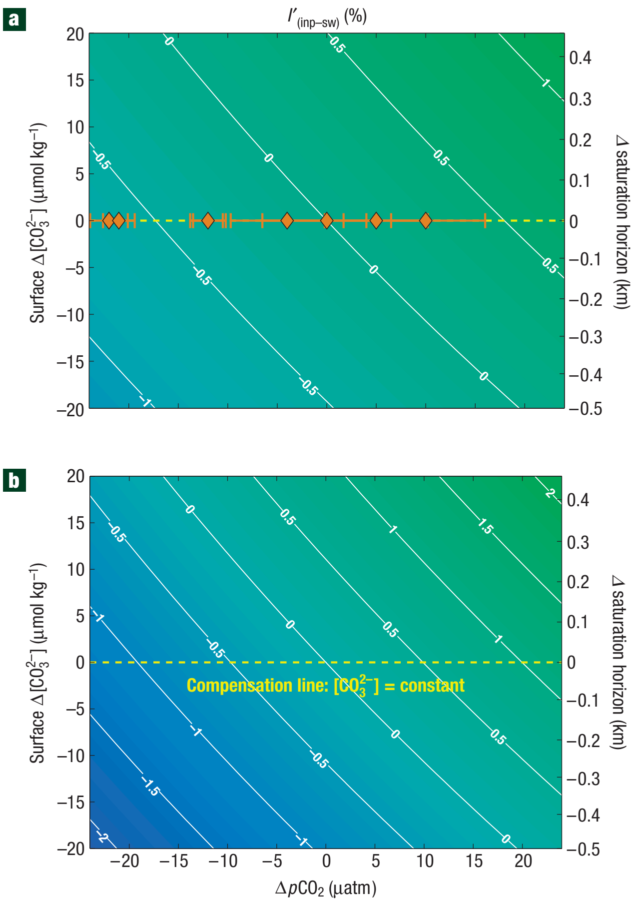

Figure 3 Sensitivity of calculated imbalance. The relative imbalance $I'_{(inp-sw)}$ (in %) refers to the mismatch between volcanism/metamorphism plus net C_{org} oxidation and silicate weathering (F_{sw}), relative to the total degassing plus C_{org} weathering flux integrated over 610 kyr (labelled white contours, equation (7)). Values show the sensitivity to long-term changes in atmospheric CO_2 (ΔpCO$_2$, bottom axis) and surface carbonate ion concentration (Δ[CO_3^{2-}], left axes). A rise and drop of [CO_3^{2-}] corresponds to deepening and shallowing of the deep-sea saturation horizon, respectively (right axes). **a**, $F_{vm} = 0.10$ Pg C y^{-1}, $F_{gw} = 0.12$ Pg C y^{-1}. Diamonds and error bars indicate linear trends and uncertainties from different fit models to the late Pleistocene CO_2 record (Table 1). **b**, $F_{vm} = 0.06$ Pg C y^{-1}, $F_{gw} = 0.06$ Pg C y^{-1}. The compensation line indicates no change in [CO_3^{2-}] and constant depth of the saturation horizon.

horizon depth by say 0.5 km, then the calculated flux imbalance is −1 to −2%. Conversely, if [CO_3^{2-}] increases, the flux imbalance is −0.2 to −0.4% of $F_{vm} + F_{gw}$. Note that despite glacial–interglacial variations, the evidence suggests a rather constant, average saturation horizon depth during the late Pleistocene[24]. Thus, the most likely scenario is constant [CO_3^{2-}]; long-term trends in saturation horizon depth larger than a few hundred metres over this timescale are very unlikely. In summary, the estimated maximum imbalance between CO_2 inputs and uptake by silicate weathering over the past 610 kyr is probably 1–2% or smaller. These are very small numbers, despite the fact that a range of possible pCO$_2$ and [CO_3^{2-}] changes have been included in our analysis (Fig. 3). Simulations with a 10-box ocean-sediment model[25] yield very similar results, which are insensitive to changes in terrestrial biomass (see the Supplementary Information).

Our results show that the net input–weathering balance closely holds on a long-term basis despite superimposed glacial–interglacial variations in CO_2, temperature and potentially weathering regimes. If weathering changes with the phase of the glacial–interglacial cycle, then net input and silicate weathering are only in balance over the timescale of a full cycle, or longer. (This impedes quantification of the imbalance on shorter timescales because the signal-to-noise ratio drops and surface recycling becomes more important.) The evidence suggests that relative to interglacial stages, weathering in the interior of continents was reduced during glacial periods, whereas weathering on exposed shelves (particularly carbonates) was enhanced owing to lowered sea level. The combined changes are believed to have been small[26,27]. Nevertheless, differences in the net input–weathering balance and ocean inventories between glacial and interglacial stages are possible. Beyond the timescale of a full glacial cycle, however, long-term trends in ocean inventories and atmospheric CO_2 require long-term trends in the endogenic imbalance (and/or surface recycling). Conversely, evaluation of scenarios solely caused by an endogenic imbalance allows the maximum mismatch between long-term carbon-cycle fluxes to be inferred from long-term trends in CO_2. In the present approach, the trends are derived from ice-core data over the past 610 kyr (Fig. 1).

The major implication of our study is that over the late Pleistocene, CO_2 inputs to the atmosphere from volcanism/metamorphism and net organic carbon oxidation were closely balanced by average continental silicate weathering uptake. Tectonically driven degassing, for instance, is entirely independent from weathering processes occurring at the surface of the Earth. The fine balance between the fluxes therefore requires an efficient stabilizing feedback that links weathering rates to, for example, volcanic degassing (coincidental agreement to within less than 1–2% over more than half a million years is implausible). The most plausible explanation is that weathering rates are regulated by a feedback controlled by the concentration of atmospheric CO_2 (refs 1–4). Previous arguments supporting the feedback were theoretical, projecting that in the absence of the feedback, significant shifts in atmospheric CO_2 would occur within a few million years. We have provided the first observational evidence for the operation and efficacy of this feedback, which reveals its essential role for stabilizing the Earth's long-term climate in recently generated ice-core CO_2 records.

METHODS

We estimated linear trends in the long-term CO_2 data using two different record lengths, two different time spacings and two different regressions, yielding eight different trend estimates (Table 1). The full and a truncated data set were analysed. For the latter, the time interval's start- and end-points were both chosen in warm periods (Marine Isotope Stage 'MIS' 15.5 and Holocene epoch) to include full wavelengths of climate cycles. The full data set includes the glacial stage preceding MIS 15.5, which may bias the trend towards the cold climate phase in the oldest part of the record. Individual time intervals between succeeding ice-core measurements are generally different, which may lead to data clustering and scarcity in different parts of the record (Fig. 1). To eliminate possible biases associated with this non-uniformity, we also used a record interpolated to uniform time spacing ($\Delta t = \text{const.}$). Trends were calculated by linear regression as well as a fit model $f(t)$ with constant, linear and periodic terms:

$$f(t) = a + b\,t + \sum_{j=1}^{4} c_j \cos[\omega_j\,(t - t_j)], \tag{8}$$

where a, b, c_j and t_j are fit parameters optimized by nonlinear least squares; ω_j are frequencies for which we used the four Milanković frequencies of 100, 41, 23 and 19 kyr.

Received 14 November 2007; accepted 27 March 2008; published 27 April 2008.

References

1. Walker, J. C. G., Hays, P. B. & Kasting, J. F. Negative feedback mechanism for the long-term stabilization of earth's surface temperature. *J. Geophys. Res.* **86**, 9776–9782 (1981).
2. Berner, R. A., Lasaga, A. C. & Garrels, R. M. The carbonate-silicate geochemical cycle and its effect on atmospheric carbon dioxide over the past 100 million years. *Am. J. Sci.* **283**, 641–683 (1983).
3. Caldeira, K. Enhanced Cenozoic chemical weathering and the subduction of pelagic carbonate. *Nature* **357**, 578–581 (1992).
4. Volk, T. Cooling in the late Cenozoic. *Nature* **361**, 123 (1993).
5. Raymo, M. E., Ruddiman, W. F. & Froelich, P. N. Influence of late Cenozoic mountain building on ocean geochemical cycles. *Geology* **16**, 649–653 (1988).
6. Francois, L. M. & Walker, J. C. G. Modelling the Phanerozoic carbon cycle and climate: Constraints from the $^{87}Sr/^{86}Sr$ isotopic ratio of seawater. *Am. J. Sci.* **292**, 81–135 (1992).
7. Bickle, M. J. Metamorphic decarbonation, silicate weathering and the long-term carbon cycle. *Terra Nova* **8**, 270–276 (1996).
8. McCauley, S. E. & DePaolo, D. J. in *Tectonic Uplift and Climate Change* (ed. Ruddiman, W. F.) 428–465 (Plenum, New York, 1997).
9. Edmond, J. M. & Huh, Y. Non-steady state carbonate recycling and implications for the evolution of atmospheric P_{CO_2}. *Earth Planet. Sci. Lett.* **216**, 125–139 (2003).
10. Petit, J. R. *et al.* Climate and atmospheric history of the past 420,000 years from the Vostok ice core, Antarctica. *Nature* **399**, 429–436 (1999).
11. Fischer, H., Wahlen, M., Smith, J., Mastroianni, D. & Deck, B. Ice core records of atmospheric CO_2 around the last three glacial terminations. *Science* **283**, 1712–1714 (1999).
12. Siegenthaler, U. *et al.* Stable carbon cycle-climate relationship during the Late Pleistocene. *Science* **310**, 1313–1317 (2005).
13. Walker, J. C. G. & Kasting, J. F. Effects of fuel and forest conservation on future levels of atmospheric carbon dioxide. *Palaeogeogr. Palaeoclimatol. Palaeoecol.* **97**, 151–189 (1992).
14. Key, R. M. *et al.* A global ocean carbon climatology: Results from GLODAP. *Glob. Biogeochem. Cycles* **18**, GB4031 (2004).
15. Dessert, C. *et al.* Erosion of Deccan Traps determined by river geochemistry: Impact on the global climate and the $^{87}Sr/^{86}Sr$ ratio of seawater. *Earth Planet. Sci. Lett.* **188**, 459–474 (2001).
16. Berner, R. A. A model for atmospheric CO_2 over Phanerozoic time. *Am. J. Sci.* **291**, 339–376 (1991).
17. Sundquist, E. T. Steady-and non-steady-state carbonate-silicate controls on atmospheric CO_2. *Quat. Sci. Rev.* **10**, 283–296 (1991).
18. Kasting, J. F. & Catling, D. Evolution of a habitable planet. *Annu. Rev. Astron. Astrophys.* **41**, 429–63 (2003).
19. Berner, R. A. & Caldeira, K. The need for mass balance and feedback in the geochemical carbon cycle. *Geology* **25**, 955–956 (1997).
20. Broecker, W. S. & Sanyal, A. Does atmospheric CO_2 police the rate of chemical weathering? *Glob. Biogeochem. Cycles* **12**, 403–408 (1998).
21. Zeebe, R. E. & Wolf-Gladrow, D. A. *CO_2 in Seawater: Equilibrium, Kinetics, Isotopes* 346pp (Elsevier Oceanography Series, Elsevier, Amsterdam, 2001).
22. Broecker, W. S. & Peng, T.-H. The role of $CaCO_3$ compensation in the glacial to interglacial atmospheric CO_2 change. *Glob. Biogeochem. Cycles* **1**, 5–29 (1987).
23. Zeebe, R. E. & Westbroek, P. A simple model for the $CaCO_3$ saturation state of the ocean: The 'Strangelove', the 'Neritan', and the 'Cretan' Ocean. *Geochem. Geophys. Geosyst.* **4**, 1104 (2003).
24. Farrell, J. W. & Prell, W. L. Climatic change and $CaCO_3$ preservation: An 800,000 year bathymetric reconstruction from the central equatorial Pacific Ocean. *Paleoceanography* **4**, 447–466 (1989).
25. Zachos, J. C., Dickens, G. R. & Zeebe, R. E. An early Cenozoic perspective on greenhouse warming and carbon-cycle dynamics. *Nature* **451**, 279–283 (2008).
26. Munhoven, G. Glacial-interglacial changes of continental weathering: Estimates of the related CO_2 and HCO_3^- flux variations and their uncertainties. *Glob. Planet. Change* **33**, 155–176 (2002).
27. Foster, G. L. & Vance, D. Negligible glacial–interglacial variation in continental chemical weathering rates. *Nature* **444**, 918–921 (2006).

Supplementary Information accompanies this paper on www.nature.com/naturegeoscience.

Acknowledgements

We thank B. Berner for reviewing the manuscript. R.E.Z. is indebted to J. Knies for providing the search expression g.rillen@loomis.hi and for discussions about organic carbon burial that sparked thinking about long-term fluxes.

Author information

Reprints and permission information is available online at http://npg.nature.com/reprintsandpermissions. Correspondence and requests for materials should be addressed to R.E.Z.